SafeDiver: Cooperative AUV-USV Assisted Diver Communication via Multi-agent Reinforcement Learning Approach

Tinglong Deng, Hang Tao, Xinxiang Wang, Yinyan Wang, Hanjiang Luo*

***Abstract*—As underwater human activities are increasing, the demand for underwater communication service presents a significant challenge. Existing underwater diver communication methods face hurdles due to inherent disadvantages and complex underwater environments. To address this issue, we propose a scheme that utilizes maritime unmanned systems to assist divers with reliable and high-speed communication. Multiple AUVs are equipped with optical and acoustic multimodal communication devices as relay nodes, providing adaptive communication services based on changes in the diver's activity area. By using multi-agent reinforcement learning (MARL) approach to control the cooperative movement of AUVs, high-speed and reliable data transmission between divers can be achieved. At the same time, utilizing the advantages of on-demand deployment and wide coverage of unmanned surface vehicles (USVs) as surface relay nodes to coordinate and forward information from AUVs, and controlling AUVs to adaptively select relay USV nodes for data transmission, high-quality communication between divers and surface platform can be achieved. Through simulation verification, the proposed scheme can effectively achieve reliable and high-speed communication for divers.**

***Index Terms*—Diving assistance, Multi-agent reinforcement learning, Maritime unmanned systems, Optical-acoustic multimodal communication, Underwater networks**

I. Introduction

As human being underwater activities increase, ensuring human safety becomes paramount. Although significant progress has been made in underwater robot technologies, human divers continue to dominate many applications due to robots' limited cognitive and executive abilities [1]. However, diving presents significant complexity and risk. Consequently, allowing divers and underwater robots to collaborate in executing marine tasks can avoid risks and improve task efficiency, which is a feasible method to solve the high-risk problem of diving [2].

In complex marine environments, divers often face constraints in both navigation and communication, which can lead to considerable safety hazards [3]. To enhance the efficiency of diving operations, reliable and high-speed communication support is essential. Currently, gestures are the primary mode of underwater communication for divers [4], but this method is limited in expressiveness and visibility. More advanced wearable and smart devices enable more comprehensive forms of communication, such as videos and images, but this communication requires high bandwidth and low latency communication systems to execute effectively.

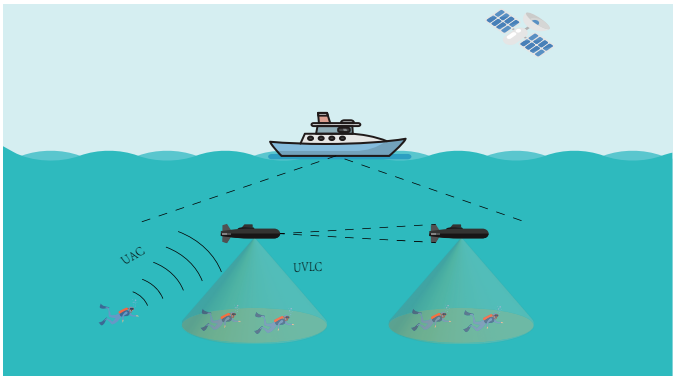

Fig. 1: A sample of underwater AUV-Diver network.

Currently, some research investigates underwater acoustic static node networks for communication [5]. However, these networks struggle to provide high-speed communication due to the inflexible configuration and face unique challenges, such as limited resources, harsh underwater condition, and unreliable acoustic communication [6]. Recently, underwater wireless optical communication (UWOC) has emerged as a promising solution for underwater communication, offering high data rates, low latency, safety, and robust immunity [7] [8]. While divers can communicate using visible light, much recent research primarily focuses on end-to-end communication [9]. To address the issue of communication range and provide better support for multiple divers, underwater wireless communication networks (UWCNs) are being explored. The use of underwater robots, such as autonomous underwater vehicles (AUVs), has become a common method for assisting divers. Currently, AUVs are primarily employed for tracking, navigation, and observation for divers [10]. Additionally, AUVs excel in data collection and transmission [11]. However, there is a notable gap in research regarding the utilization of the autonomous mobility of multi-AUV to enhance communication for divers.

Although AUVs have many advantages in underwater exploration, AUV based maritime communication networks are constrained by several factors, such as limited transmission power and sensing range, and spectrum resources [12]. With the rapid development of marine internet of things (MIoT), unmanned surface vehicles (USVs) have attracted widespread attention

Tinglong Deng, Hang Tao, Xinxiang Wang, Yinyan Wang, and Hanjiang Luo are with College of Computer Science and Engineering, Shandong University of Science and Technology, Qingdao, China.
Corresponding author: Hanjiang Luo, Email: hjluo@sdust.edu.cn.

in scientific research and ocean application development due to their advantages of on-demand deployment, wide sensing coverage, and the ability to serve as sea-air bridges [13]. At the same time, USVs have the advantages of high maneuverability and long endurance, which can undertake long-term marine environmental monitoring tasks. They can also directly collect data and use Radio Frequency (RF) to transmit to surface platform, providing an opportunity to reduce data transmission delays [14].

Recently, the rapid advancement in multi-agent reinforcement learning (MARL) has opened up new possibilities for improving the efficiency of underwater robotic operations through collaboration [15]. Unlike traditional methods that rely on intricate mathematical models, reinforcement learning (RL) accumulates knowledge through ongoing interactions with the environments. However, the ability and efficiency of a single agent to perform tasks are relatively low. Therefore, multi-agent systems have been introduced to work cooperatively with multiple agents [16]. MARL has greater advantages over other intelligent algorithms in terms of integrity, stability, and robustness in maritime applications [17].

Inspired by those previous works, we propose a scheme that utilizes maritime unmanned systems to assist divers for communication. We utilize AUVs as relays in UWCNs, which can provide mobile coverage based on the location change of divers. At the same time, we combine the complementary advantages of optical-acoustic multimodal communication to further improve communication quality. Finally, we propose a multi-agent cooperative movement algorithm based on multi-agent proximal policy optimization (MAPPO) [18], and combine it with a clustering algorithm to perform cooperative movement according to the position changes of divers, so as to provide stable communication service for divers. At the same time, by deploying USV nodes on the sea surface to forward information from AUVs, the multi-agent delayed deterministic policy gradient (MATD3) [19] based algorithm is used to adaptively control the dynamic relay node selection of AUVs based on the position changes of AUVs and USVs, achieving efficient communication between divers and surface platform. The contributions of this paper are summarized as follows.

- We propose an innovative multi-AUV-assisted diver communication scheme that combines the advantages of optical-acoustic multimodal communication to address the limitation of high-speed communication between divers.
- We propose an USV-AUV assisted communication method to address the issue of limited communication between divers and surface platform.
- We also conduct extensive simulations to evaluate the effectiveness of the proposed scheme.

The rest of the paper is organized as follows. Section II reviews the related work. Section III provides the system model. Section IV provides a detailed description of the assisted diver underwater communication scheme design. Section V presents the USV-AUV assisted communication method. We conduct simulations to validate the proposed solution in Section VI. Finally, we conclude the paper in Section VII.

II. Related Work

Many maritime works require divers, but divers are easily affected by the underwater environments, sometimes causing serious consequences. Therefore, how to use underwater robots and wireless communication networks to improve the safety and task execution efficiency of divers is a critical issue that needs to be addressed. Edge et al. [20] proposed a diver interest pointing algorithm in which AUV infers key areas by recognizing the diver's direction and improving the efficiency of human-machine collaboration. Vivekanand et al. [21] proposed a diver monitor system to monitor the physical condition of divers. If any abnormal situation occurs with the diver, a Save our Souls (SOS) message and the diver's global positioning system (GPS) location can be sent. Bernardi et al. [5] proposed a new type of underwater acoustic network diving operation system, which utilizes surface buoy nodes, underwater static nodes, and diver nodes to form an underwater wireless acoustic network. However, this system is only applicable to fixed areas and lacks autonomy and scalability. Anjangi et al. [22] used surface nodes and diver nodes to form a static underwater acoustic network to realize communication between divers. Luo et al. [23] proposed a reliable optical communication transmission scheme to cope with ocean interference, which utilizes a deep reinforcement learning approach to adjust the buoy beam direction and control the movement of the unmanned aerial vehicle to maintain stable data transmission via an optical link. Zhang et al. [24] proposed an underwater wireless sensor network (UWSN) scheme based on UWOC, which uses a dual hop system to expand the coverage area of UWSN with mobile nodes, and can use visible light to achieve communication between underwater diver nodes and other mobile nodes.

Introducing USV as a mobile air to underwater relay assisted transmission is a common solution in maritime wireless communication systems. In recent years, USV have made significant progress in motion control, obstacle avoidance, path planning, and other areas, which can meet the requirements of various applications at maritime [25]. Wang et al. [26] provided an overview of USV assisted maritime wireless communication by introducing some typical USV application scenarios, basic network architectures, design considerations, and main challenges. Taking USV assisted mobile relay as an example, they demonstrated the advantages of using USV in maritime wireless communication. Su et al. [27] considered a USV assisted ocean data collection network with the goal of minimizing energy consumption and data loss, where USVs collect data from multiple monitoring terminals while avoiding collisions. Hu et al. [28] proposed a data transmission security scheme assisted by USVs, which protects the security of sea air cross domain data transmission by interfering with eavesdropping AUVs. Han et al. [29] designed a USV-AUV communication scheme that achieves a dynamic relay access process by minimizing transmission costs under end-to-end delay constraints. In this paper, we design a maritime unmanned systems to assist divers in communication, which provides reliable and high-speed communication services to divers.

III. System model

In this section, we provide the communication channel models, which include underwater visible light communication (VLC) channel model, underwater acoustic channel model and radio frequency channel model.

A. Underwater VLC Channel Model

The path loss of underwater VLC is composed of attenuation loss and geometric loss. In the scenario of underwater LED diffuse light signal propagation, only nodes in the line-of-sight (LOS) can receive the signal. According to the widely accepted Beer-Lambert law, the attenuation loss of underwater visible light can be expressed as [30]

$$PL_{BL}(d) = 10\log_{10}(e^{-cd}), \tag{1}$$

where d is the link range between the transmitter and receiver, and c is the extinction coefficient. The extinction coefficient can be determined by the absorption coefficient a and the scattering coefficient b, which can be expressed as $c = a + b$.

For diffuse and semi-collimated light sources such as LED, it is necessary to consider the influence of geometric loss. So geometric loss can be mathematically expressed as [30]

$$PL_{\mathrm{G}}(d) \approx 10\log\left(\left(\frac{D_R}{\theta_{1/e}d}\right)^2\right), \tag{2}$$

where D_R and $\theta_{1/e}$ are the receiver aperture diameter and full width transmitter beam divergence angle, respectively.

By combining the path loss caused by attenuation and geometric loss, we can obtain the total path loss, which is mathematically expressed as follows.

$$\begin{aligned} PL(d) &= PL_{BL}(d) + PL_{\mathrm{G}}(d) \\ &\approx 10\log_{10}\left(\left(\frac{D_R}{\theta_{1/e}d}\right)^2 e^{-cd}\right). \end{aligned} \tag{3}$$

The SNR of communication can be expressed as

$$SNR = \frac{\eta^2 R^2 h^2 P_T}{\sigma_n^2}, \tag{4}$$

where η is the electrical to optical conversion efficiency of a diode, R is the responsivity of the photodetector, P_T is the transmit power, σ_n^2 is the noise variance and $h = 10^{PL(d)/10}$ denote the optical channel coefficient.

According to Shannon's theorem, the maximum data transmission rate of the channel can be expressed as

$$C = B\log_2(1 + SNR), \tag{5}$$

where B is the bandwidth.

The theoretical bit error rate (BER) of on-off keying (OOK) can be expressed as

$$BER = \mathcal{Q}\left(\sqrt{\frac{SNR}{2}}\right), \tag{6}$$

where $\mathcal{Q}(\cdot)$ is the tail probability of the standard normal distribution.

B. Underwater Acoustic Channel Model

The power loss of underwater acoustic signals mainly consists of geometric spreading and geometric absorption, which can be expressed as [31]

$$L(d, f) = L_s(d) + d_k L_a(f), \tag{7}$$

where d is the distance, f is the frequency, $L_s(d)$ is the geometric spreading loss when distance from source is d meters, $d_k = d \times 10^{-3}$ is the distance in km, and $L_a(f)$ is the geometric absorption loss per [dB/km] at f kHz frequency.

The geometric spreading loss can be specifically expressed as

$$L_s(d) = k \times 10\log(d), \tag{8}$$

where $k \in [1, 2]$ is the exponent that describes the geometric spreading; when $k = 1$ and $k = 2$, represent as a cylindrical spreading and spherical spreading, respectively.

The geometric absorption loss is commonly expressed using Thorp's empirical formula [31], which is derived from ocean measurement data as follows.

$$L_a(f) = 0.11\frac{f^2}{1+f^2} + \frac{44f^2}{4100+f^2} + 3\times10^{-4}f^2 + 3.3\times10^{-3}. \tag{9}$$

The power loss can also be expressed as

$$L(d, f) = 10\log(P_r/P_s), \tag{10}$$

where P_r and P_s are receive power and transmit power, respectively.

Given the underwater acoustic receive power P_r, the SNR can be expressed as

$$SNR = \frac{P_r}{N(f)\Delta f}, \tag{11}$$

where $N(f)$ and Δf represent the interference noise and the bandwidth of the receiver, respectively.

C. Radio Frequency Channel Model

The path loss of RF in free space refers to the signal attenuation caused by the spatial diffusion of electromagnetic waves. The path loss of communication between USV and surface platform can be expressed

$$PL_{rf} = 32.44 + 20\log d_r + 20\log f_r, \tag{12}$$

where d_r and f_r are the distance and frequency in RF communication, respectively.

For the RF link between USV and surface platform, we consider Rayleigh fading as a representation of sea surface reflection [29], and the probability density function of Rayleigh distribution can be expressed as

$$p(x) = \frac{x}{\delta^2}e^{-\frac{x^2}{2\delta^2}}, \tag{13}$$

where δ is the scaling parameter.

The channel power gain of RF communication between USV and surface platform can be expressed as [32]

$$G_{rf} = \left[(G_t \times G_r \times \xi) \,/\, \left(16\pi^2(d_r/d_0)^2\right)\right] \times R_a, \tag{14}$$

where G_t is the transmitter antenna gain, G_r is the receiving antenna gain, d_0 is a far field reference distance, ξ is carrier wavelength, R_a is Rayleigh distributed.

The RF communication unit power can be expressed as

$$SNR = \frac{G_{rf}}{N_0}, \tag{15}$$

where N_0 is the noise power.

IV. Multi-AUV Assisted Diver Communication

In this section, we first provide a general description of proposed method and the communication problem analysis. Then, we present a diver clustering algorithm to divide the divers into clusters. Finally, we design a multi-AUV cooperative movement algorithm to perform AUV assisted diver communication.

A. General Description

We consider a communication network based on multi-AUVs and divers, which consists of N AUVs, M divers, and an USV. M divers perform underwater tasks and use AUV-assisted positioning technology to determine their positions [10]. Multi-AUV with cameras and sensors are configured to assist underwater tasks above the divers. AUVs mainly serve as mobile communication relay nodes, enabling communication between divers, while also collecting and forwarding surrounding environmental information. At the same time, they also need to forward information from an USV or a surface platform. As shown in Fig. 1, divers within the visible light communication range can use VLC, otherwise underwater acoustic communication (UAC) is used. When divers are served by two different AUVs, VLC between AUVs is also required. In a multimodal network, AUVs and divers need to be equipped with both LED and UAC equipment to ensure high-speed data transmission by utilizing the complementary optical-acoustic multimodal communication [33]. Specifically, VLC is used for high-speed data transmission at a close distance, while UAC is used for long-distance data transmission at a low speed. The USV acts as a relay node on the water surface which is responsible for communication between divers and base stations.

The multi-AUV assisted diver communication architecture is shown in Fig. 2. It mainly includes two modules: multi-AUV cooperative movement and K-medoids clustering. The purpose of multi-AUV cooperative movement is to maximize communication coverage for divers. In K-medoids clustering module, in order to optimize this coverage problem, we utilize the K-medoids approach to cluster divers and find the centroid position of each cluster, which is used as the target position for multi-AUV cooperative movement. The K-medoids can eliminate the interference of outliers and the calculation process is not complicated, making it suitable for combining with MARL algorithm. In the multi-AUV cooperative movement module, we map the entire process to POMDP and propose a multi-AUV cooperative movement strategy based on MAPPO approach to control the swarm of AUVs.

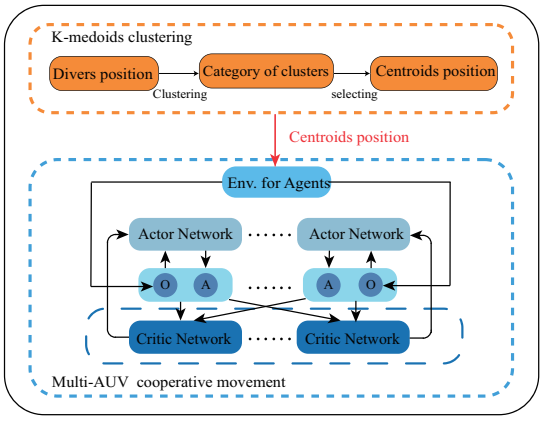

Fig. 2: The illustration of multi-AUV assisted diver communication architecture via MARL.

B. Problem Analysis

We need to analyze the scope of optical-acoustic multi-modal communication to determine when using VLC and UAC can maximize communication quality. The AUV needs to act as a mobile communication relay to assist divers in transmitting images, videos, and other necessary information between them. Due to divers' need to apply high-speed and reliable communication, we adopt an optical-acoustic multimodal communication method to improve the speed of data transmission. Consequently, multi-AUV need to choose appropriate movement strategies to achieve maximum VLC coverage for multiple divers. At the same time, the AUV needs to determine the scope of optical-acoustic communication based on specified communication requirements.

As a relay node, the AUV acts as both a transmitter and receiver, and the communication between divers is multi-hop. The BER_E considering all the links can be expressed as

$$BER_E = 1 - \prod_{i=1}^{\mathcal{N}}(1 - BER_i), \tag{16}$$

where $\mathcal{N}$ is the number of link, and BER_i is the BER of the i-th link.

Based on (6), the SNR_{req} that satisfies a given target BER $\mathcal{T}$ can be expressed as

$$SNR_{req} = 2(\mathcal{Q}^{-1}(\mathcal{T}))^2. \tag{17}$$

The maximum link distance that satisfies $\mathcal{T}$ can be expressed as

$$d_{\max} = \left[\frac{\mathrm{W}\left(\frac{c}{2}(1-T)\left(\frac{D_{\mathrm{R}}}{\theta_{1/e}}\right)\left(\sqrt{\frac{2\sigma_n^2}{R^2\eta^2 P_T}}\mathcal{Q}^{-1}\mathcal{T}\right)^{\left(\frac{T-1}{2}\right)}\right)}{\frac{c}{2}(1-T)\left(\frac{D_{\mathrm{R}}}{\theta_{1/e}}\right)^T} \right]^{\frac{1}{1-T}}, \tag{18}$$

where T is a correction coefficient which determined by fitting data, $W(x)$ is the Lambert-W function [30].

Thereby, the maximum full-width beam divergence angle $\theta_{1/e}^{max}$ at a specified $\mathcal{T}$ can be derived, which can be expressed

as

$$\theta_{1/e}^{max} = \sqrt{\frac{\sqrt{P_T} R D_R^2 \eta e^{-cd}}{\sqrt{2\sigma_n^2} d^2 \mathcal{Q}^{-1}\mathcal{T}}}. \tag{19}$$

When the link distance is fixed, the LED light source of the AUV and the diver have the same maximum beam divergence angle. At this time, when the AUVs and divers work at fixed depths, the maximum beam divergence angle $\theta_{1/e}^{max}$ can be obtained based on the link distance d. When the diver's position is outside the maximum beam divergence angle, only UAC can be used; when the diver's position is concentrated within the range of the beam divergence angle, bidirectional VLC can be achieved. As AUVs work at a fixed depth and AUVs can be aligned to reduce the constraint of beam divergence range [34], the communication limitation mainly lies in the link distance d between AUVs.

C. Underwater Diver Clustering Algorithm

The relative position between the AUV and the diver determines the performance of the communication link. The AUV can obtain the position information of the diver through sensors [10], but the position of multiple divers can change at any time, making it difficult for the AUV to provide high-quality communication service for divers. To optimize this problem, we adopt the K-medoids clustering algorithm [35], dividing the divers into N clusters based on their positions, and then N AUVs cooperative move to the centroid position of each cluster to maximize the diver's communication coverage service.

In this study, one of the objectives is to maximizing VLC service quality. To achieve this, we need to eliminate the interference from certain outliers during the clustering process and when selecting centroids for divers. The K-medoids algorithm is advantageous because it is not sensitive to outliers and selects centroids from existing data points, making it a fast and efficient method.

Assume that the diver set $D = \{m_1, m_2, ..., m_M\}$ contains M divers. The Euclidean distance $dist$ from the j-th non-centroid diver to the centroid of the i-th cluster W_i can be expressed as

$$dist(W_i, m_j) = \sqrt{\sum_{t=1}^{l} (W_{i_t} - m_{j_t})^2}. \tag{20}$$

Randomly select K divers from D as centroid W during initialization, where $W = \{W_1, W_2, ..., W_K\} \subseteq D$, and then assign other divers to the nearest centroid based on the distance, then K clusters $C_1, C_2, ..., C_K$ are formed to minimize the total cluster cost E, which can be expressed as

$$E = \sum_{k=1}^{K} \sum_{p \in C_k} dist(W_k, p)^2, \tag{21}$$

where this cost function evaluates the average dissimilarity between the diver and its centroid. The detailed algorithm steps are shown in Algorithm 1.

Algorithm 1 The Diver K-medoids Algorithm.

1: In the initial stage, randomly select K divers from the total M divers as centroids.
2: **Repeat**
3: Base on (20), assign the remaining divers to the cluster represented by the current best centroid.
4: Select non-centroid divers in order within each cluster.
5: Base on (21), calculate the cost value E when the new diver becomes centroid.
6: Then select the diver with the smallest cost E as the new centroid.
7: **until** all centroids no longer change or the set maximum number of iterations has been reached.

D. Multi-AUV Cooperative Movement Algorithm

We design the algorithm based on MAPPO to achieve cooperative movement of multi-AUV and realize high-speed communication between divers. During the training phase, the input of the value function is the observations of all agents, while during the execution phase, the action function only outputs actions based on its own observations. Firstly, we need to map the above problem to POMDP, which is represented by a five-tuple $(\mathcal{S}, \mathcal{O}, \mathcal{A}, \mathcal{R}, \mathcal{P})$ as follows.

- State Space: $\mathcal{S} = \{s_1, s_2, \cdots, s_N\}$ is all possible state spaces of N agents, which is the set of states for all agents, where the state space of AUV$_i$ is $s_i = (x_i, y_i, u_i, v_i, r_i)$, x_i, y_i denote the positions of AUV$_i$ on the X- and Y-axis, respectively. And $u_i, v_i, r_i \in \mathbb{R}$ represents surge, sway and yaw angular velocity of AUV$_i$, respectively.
- Observation Space: $\mathcal{O} = \{o_1, o_2, \cdots, o_N\}$ is the set of observation space for all AUVs, where o_i is the partial observation information obtained by AUV$_i$ from the global state. In partially observable model, the information that AUVs can observe $o_i = \{x_i, y_i, \boldsymbol{v_i}, \boldsymbol{d_m}, \boldsymbol{d_a}\}$, where x_i, y_i is the position of AUV$_i$, $\boldsymbol{v_i}$ is velocity vector of AUV$_i$, $\boldsymbol{d_m}$ and $\boldsymbol{d_a}$ are vectors of distance from all centroids and other AUVs to AUV$_i$, respectively.
- Action Space: $\mathcal{A} = \{a_1, a_2, \cdots, a_N\}$ is the set of action space for all AUVs. The action set of AUV$_i$ is represented by $\boldsymbol{a_i} = (a_i^u, a_i^v, a_i^r)$, where $a_i^u, a_i^v, a_i^r \in \mathbb{R}$ represent the surge, sway and yaw angular velocity by thrust control signals of AUV$_i$, respectively. Furthermore, the kinematics model of AUV is as follows [36].

$$\eta = JV, \tag{22}$$

$$J = \begin{bmatrix} cos\psi & -sin\psi & 0 \\ sin\psi & cos\psi & 0 \\ 0 & 0 & 1 \end{bmatrix}, \tag{23}$$

where ψ is the yaw angular, $\eta = [x, y, \psi]^T$ and $V = [u, v, r]^T$ are the state vectors of interial reference frame (IRF) and the body-fixed reference frame (BRF), respectively.

- Reward: $\mathcal{R} = \{r_1, r_2, \cdots, r_N\}$ is the reward of all AUVs. The reward function represents the immediate

reward received by each AUV for executing actions in its current state. Based on the clustering results, we use the centroid of each cluster as the moving target for all AUVs. Specifically, each AUV will receive rewards based on the sum of the minimum distances closest to each centroid, which can be expressed by

$$r_i = -\sum_{i=1}^{N} \min_{1 \le j \le N} \left(\sqrt{(\boldsymbol{q_i} - W_j)^2} \right), \tag{24}$$

where $\boldsymbol{q_i}$ denoted the location of AUV$_i$.

- State Transition Function: the state transition function $\mathcal{P}$ is the probability form the current state $\mathcal{S}$ to the next state $\mathcal{S}'$ under action $\mathcal{A}$, expressed as

$$\mathcal{P} : \mathcal{S} \times \mathcal{A} \to \mathcal{S}'. \tag{25}$$

The MAPPO algorithm is based on the centralized training and decentralized execution (CTDE) framework, and the CTDE is actually a compromise between fully centralized and fully decentralized, as it preserves some global information and has stronger applicability. When training the actor network, it only trains based on its own observations o_i, but when training the critic network, it requires the collection of observations by all agents, represented by

$$\mathbf{x} = \{o_1, o_2, ..., o_N\}. \tag{26}$$

The PPO algorithm is based on the Actor-Critic framework and has two neural networks π and V to simulate the action-value function and state-value function, where θ and ω are their network parameters, respectively. The generalized advantage estimator (GAE) [37] is represented as

$$A_t = \sum_{l=0}^{P} (\gamma\lambda)^l \delta_{t+l}, \tag{27}$$

where $\delta_t = r_t + \gamma V(s_{t+1}) - V(s_t)$ is the TD error at step t, P is the step number which is a hyperparameter, γ is the discount factor, and λ is the GAE parameter. The policy loss can be expressed as

$$\mathcal{L}(\theta) = \mathbb{E}_t \left[\min \left(\rho_t(\theta) A_t, \operatorname{clip} \left(\rho_t(\theta), 1-\epsilon, 1+\epsilon \right) A_t \right) \right], \tag{28}$$

$$\rho_t(\theta) = \frac{\pi_\theta \left(a_t \mid s_t \right)}{\pi_{\theta_{\text{old}}} \left(a_t \mid s_t \right)}, \tag{29}$$

where $\rho_t(\theta)$ is the ratio of the new policy to the old policy, and ϵ is a hyperparameter that represents the range of clip.

The critic network is used to evaluate the output of the actor network, it can be updated according to the following loss function

$$\mathcal{L}(\omega) = \mathbb{E}_t \left[(V_\omega(s_t) - y(t))^2 \right]. \tag{30}$$

The main characteristic of MAPPO is that it has a centralized value function inputs, which means that during the training phase, all agents observations are used as inputs, and the loss function during the centralized training phase can be expressed as

$$\mathcal{L}(\omega_i) = \mathbb{E}_{\mathbf{x},a,r,\mathbf{x}'} \left[(Q(\mathbf{x}, a_1, ..., a_N) - \mathrm{y})^2 \right], \tag{31}$$

$$\mathrm{y} = r_t + \gamma Q(\mathbf{x}', a_1', ..., a_N'), \tag{32}$$

where Q is the centralized value function.

During the execution phase, each agent executes in a distributed manner based on its own observation. The final policy loss for each agent can be expressed as

$$\mathcal{L}(\theta_i) = \mathcal{L} + \lambda_{entropy} \mathcal{H}(\pi_{\theta_i}), \tag{33}$$

$$\mathcal{L} = \mathbb{E}_{X \sim \mathcal{D}} \left[\min \left(\rho_t^i(\theta) A_t^i, \operatorname{clip} \left(\rho_t^i(\theta), 1-\epsilon, 1+\epsilon \right) A_t^i \right) \right], \tag{34}$$

where $\mathcal{D}$ is experience replay buffer used to store data, which stores tuple $(\mathbf{x}, \mathbf{x}', a_1, ..., a_N, r_1, ..., r_N)$, $\mathcal{H}(\pi_{\theta_i})$ denotes the entropy of policy π_{θ_i}, and $\lambda_{entropy}$ is a hyperparameter. The complete algorithm process is summarized in Algorithm 2.

Algorithm 2 Multi-AUV Cooperative Movement Algorithm.

```
Randomly initialize the Actor and Critic networks of each agent with random network parameters θ_i and ω_i.
Initialize experience replay buffer D.
for episode = 1 → E do
    Clustering divers using Algorithm 1.
    Obtain initial observations x of all AUVs.
    for t = 1 → T do
        For each AUV, select an action a_i = π_{θ_i}(o_i) using the current strategy.
        Execute action a = (a_1, ··· , a_N) and obtain reward r = (r_1, ··· , r_N) and next observation x'.
        Store (x, a, r, x') into the replay buffer D.
        Randomly sample some tuple from D using the size of batchsize S.
        For each AUV, calculate the A_t^i using the critic network Q_{ω_i} and update their actor network π_{θ_i} based on (33,34).
        For each AUV, update their critic network Q_{ω_i} based on (31,32).
    end for
end for
```

V. USV-assisted Communication Method

In this section, we present the design of USV assisted communication method. We first describe the problem analysis. Then we present the algorithm based on MATD3, in which AUV can dynamically select suitable an USV as relay node to forward information to surface platform based on its own and the USV positions while covering communication with divers.

A. Problem Analysis

As shown in Figure 3, we consider an UAV assisted communication scenario, which consists of a surface platform, $\mathcal{M}$ USVs, N AUVs, and M underwater divers. Divers are distributed in underwater areas to execute exploration and other tasks, and use AUVs as relay nodes to transmit information between each other through optical-acoustic multimodal communication. AUV provides communication services for divers through cooperative movement. However, cross-media

communication between AUVs and surface platform is highly susceptible to limitations, such as limited communication range, low bandwidth, and high latency. In this case, USVs need to be used as surface nodes to assist in forwarding information. The AUV and USV transmit information through a low bandwidth UAC link underwater, while the USV and surface platform use a high bandwidth RF link to transmit information. The set of N AUVs is represented as $A_\upsilon = \{\upsilon_1, \upsilon_2, ..., \upsilon_N\}$, and the set of $\mathcal{M}$ USVs is represented as $A_u = \{u_1, u_2, ..., u_\mathcal{M}\}$. The surface platform is represented as u_0. Assuming that in a time slot t, the transmission data volume of all AUVs follows a Poisson distribution, expressed as $\Theta(t) = \{q_{\upsilon_i}(t) | q_{\upsilon_i}(t) \sim \boldsymbol{P}(t), \upsilon_i \in A_\upsilon\}$.

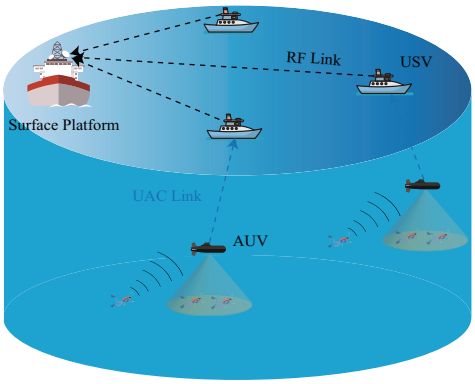

Fig. 3: Illustration of USV assisted communication.

When AUV υ_i selects USV u_j as the relay node to forward information to the platform, the entire transmission process can be divided into two stages, $\upsilon_i - u_j$ and $u_j - u_0$. The achievable transmission rate when υ_i transmitting information to the selected relay node u_j through UAC link in time slot t is [29]:

$$R_{i,j} = b\theta_{i,j}\log_2\left(1 + \frac{p_a}{bH_{i,j}(t)N(f)}\right), \tag{35}$$

where b is the channel bandwidth, $\theta_{i,j}$ is the selection variables for AUV υ_i and USV u_j , if $\theta_{i,j} = 1$ represents that relay node u_j is selected to forward message from υ_i at the time slot t, if $\theta_{i,j} = 0$, it represents u_j is not selected by υ_i, p_a is the transmit power of AUV υ_i, $H_{i,j}(t)$ denotes the path loss between υ_i and u_j at time slot t.

Considering the issue of load balancing, each USV relay can be selected by at most one AUV at a time slot. For the RF link between chosen relay u_j and the surface platform u_0, we consider the Rayleigh fading as the channel model. Therefore, the achievable transmission rate of the relay node USV u_j selected by the AUV υ_i to the surface platform u_0 at the time slot t can be expressed as

$$R_{j,0}^{(i)} = b_r\log_2\left(1 + \frac{p_u G_{j,0}^{(i)}(t)}{b_r N_0}\right), \tag{36}$$

where b_r is bandwidth of RF link, p_u is the transmit power of USV u_j, N_0 is the spectrum density of the noise, $G_{j,0}^{(i)}(t)$ is the channel power gain between u_j and u_0 at time slot t.

Based on the above description, the total transmission energy consumption at υ_i can be expressed as

$$EM_i = \theta_{i,j}(t)p_a \boldsymbol{t}_{i,j}^{s,u}(t) + p_u \boldsymbol{t}_{j,0}^{u,d}(t), \tag{37}$$

where $\boldsymbol{t}_{i,j}^{s,u}(t) = \frac{q_{\upsilon_i}(t)}{R_{i,j}(t)}$ and $\boldsymbol{t}_{j,0}^{u,d}(t) = \frac{q_{\upsilon_i}(t)}{R_{j,0}^{(i)}(t)}$ represents the time cost of two stages of collaborate transmission.

The reliability and speed of communication mainly depend on the relative positions between AUVs and relay nodes. Therefore, dynamic relay node selection by AUVs, based on their own positions and USV positions, is key to ensuring efficient collaborative communication. Unlike prior studies focused on short-term USV-AUV deployment in fixed locations or isolated data transmission, we propose a long-term dynamic relay selection method for cross-media collaborative communication, optimized based on real-time AUV and USV positions. The mobility of AUVs and USVs leads to dynamic channel conditions, causing the optimal matching relationship between them to change over time. In each time slot, each AUV can be paired with only one USV for data transmission, while each USV can forward data from at most one AUV to avoid bandwidth contention. Consequently, multiple AUVs must collaboratively select relay nodes to maximize the overall communication rate. Thus, we formulate the optimization objective as maximizing the long-term overall communication rate, expressed as

$$\begin{aligned} &\max \frac{1}{N}\sum_{i=1}^{N} R_i(t) \\ &s.t. \sum_{i=0}^{N} \theta_{i,j}(t) = 1, \forall i \in A_\upsilon \\ &\sum_{i=0}^{N} \theta_{i,j}(t) <= 1, \forall j \in A_u. \end{aligned} \tag{38}$$

B. Multi-AUV Dynamic Selection Algorithm

In order to maximize the cross-media communication data transmission rate of AUV, we propose a dynamic node selection algorithm based on MATD3. This algorithm is based on the CTDE architecture, so the dynamic node selection problem can be modeled as a POMDP represented by tuples $(\tilde{S}, \tilde{O}, \tilde{A}, \tilde{P}, \tilde{R})$.

- State Space: $\tilde{S} = \{\tilde{s}_1, \tilde{s}_2, \cdots, \tilde{s}_N\}$ is all possible state spaces of N agents, which is the set of states for all agents. The position changes of USV and AUV will affect the selection of relay nodes for AUV, and it is also necessary to understand the selection situation of each relay node. Therefore, the state space of AUV υ_i represents as

$$\tilde{s}_i = (\mathrm{P}_i^s, q_{s_i}, \mathrm{P}_u, \mathrm{P}_0, \varpi), \tag{39}$$

  where P_i^s denotes the position of AUV υ_i, q_{s_i} denote the amount transmission data, P_u denotes position of all USVs, P_0 is the position of surface platform, ϖ is a matrix representing whether each USV relay node is selected or not.
- Observation Space: $\tilde{O} = \{\tilde{o}_1, \tilde{o}_2, \cdots, \tilde{o}_N\}$ is the set of observation space for all AUVs. In POMDP, each AUV

can only observe partial information from the global state. The observation space $\tilde{o}_i$ of AUV υ_i can be expressed as

$$\tilde{o_i} = \left(d_i^{s,u}, d_i^{s,s}, d_i^{s,0}, \varpi_i^s, q_{s_i}\right), \tag{40}$$

where $d_i^{s,u}$, $d_i^{s,s}$and d_i^0 denotes the distance vector between AUV s_i and all USVs, other AUVs and surface platform u_0 respectively, ϖ_i^s denotes the information of USVs selected by other AUVs.

- Action Space: $\tilde{A} = \{\tilde{a}_1, \tilde{a}_2, \cdots, \tilde{a}_N\}$ is the set of action space for all AUVs. The main purpose of dynamic relay node selection is to improve the data transmission rate of AUVs by selecting appropriate relay USVs. Therefore the action $\tilde{a}_i$ of AUV υ_i can be represented as

$$\tilde{a}_i = (\delta_{i,j}), \tag{41}$$

where $\delta_{i,j}$ denotes the selection variables for AUV and USV. If $\delta_{i,j} = 1$ represents AUV υ_i selecting the jth USV u_j as a relay node to transmit data. AUV υ_i needs to select any USV for data transmission at the time slot, so the action needs to meet the following

$$\sum_{j=0}^{\mathcal{M}} \delta_{i,j} = 1. \tag{42}$$

- Reward: $\tilde{R} = \{\tilde{r}_1, \tilde{r}_2, \cdots, \tilde{r}_N\}$ is the reward of all AUVs. We utilize the total transmission time of all AUVs as a reward signal to enable AUVs to dynamically select transmission nodes correctly and improve transmission rate. The reward $\tilde{r}_i$ of AUV υ_i can be represented as

$$\tilde{r}_i = \mu_1 \left(-\sum_{i=1}^{n} \left(\boldsymbol{t}_{i,j}^{s,u} + \boldsymbol{t}_{j,0}^{u,d} \right) \right) + \mu_2 r_c, \tag{43}$$

where μ_1 and μ_2 are hyperparameters representing weights, r_c is the reward of load balance, which means AUV receive a negative reward when it selects a relay node that has been selected by another AUV. The reward function can guide all AUVs to collaboratively select USV nodes with less transmission time.

- State Transition Function: the state transition function $\tilde{P}$ denotes the probability form the current state $\tilde{S}$ to the next state $\tilde{S}'$ under action $\tilde{A}$, expressed as

$$\tilde{P} : \tilde{S} \times \tilde{A} \to \tilde{S}'. \tag{44}$$

MATD3 is an extension of TD3 in multi-agent systems. It combines the stability enhancement mechanism of TD3 and applies it to multi-agent systems, enabling them to perform better in mixed collaborative and competitive environments. The Actor-Critic architecture is adopted in the MATD3 algorithm, where each agent consists of three networks: an Actor network $\tilde{\pi}_{\tilde{\phi}}$ with parameters $\tilde{\phi}$ and two Critic networks $\tilde{Q}_{\tilde{\theta}_1}$, $\tilde{Q}_{\tilde{\theta}_2}$ with parameters $\tilde{\theta}_1$ and $\tilde{\theta}_2$. The role of the Actor network is to take actions based on observations, while the Critic network is responsible for evaluating actions and preventing overestimation issues in a single Critic framework. In addition, target Actor and Critic networks with parameters $\tilde{\phi}'$ and $\{\tilde{\theta}_i'\}_{i=1,2}$ are used to stabilize the training process. The value function of the m-th agent can be expressed as [38].

Algorithm 3 Multi-AUV Dynamic Selection Algorithm.

```
Initialize the Actor and Critic networks of each agent with random network parameters φ̃_m and θ̃_m.
Initialize target networks θ̃'_{m,i} ← θ̃_{m,i} and φ̃'_i ← φ̃_i .
Initialize experience replay buffer D̃.
for episode = 1 → Ẽ do
    Initial observation set x̃ of all AUVs.
    for t = 1 → T̃ do
        For each AUV, select an action with exploration noise ã_m = π̃_{φ̃_m}(õ_m) + ψ
        Observe new sate information x̃' and get reward R̃
        Store transition tuple into the replay buffer D̃.
        for AUV m = 1 → N do
            Sample a random mini-batch of S̃ samples from D̃.
            For each AUV, update their critic network according to (48).
            if t mod κ then
                For each AUV, update their Actor network according to (47).
                Update the three target networks according to (51).
            end if
        end for
    end for
end for
```

$$\tilde{Q}_{\tilde{\theta}_{m,i}}(\tilde{\mathbf{x}}, \tilde{a}_1, \cdots, \tilde{a}_N) = \mathbb{E}_{\tilde{r},\tilde{\mathbf{x}}} \left[\tilde{r}_m + \tilde{\gamma} \tilde{Q}_{\tilde{\theta}'_{m,i}}(\tilde{\mathbf{x}}', \tilde{a}_1', \cdots, \tilde{a}_N') \right], \tag{45}$$

where i=1,2 denotes two Critic networks, $\tilde{\mathbf{x}}$ denotes the set of state information for all agents, $\tilde{\gamma}$ is the discount factor. To address the issue of overestimation in single Critic networks, the objective value function be updated to

$$\tilde{y}_m = \tilde{r}_m + \tilde{\gamma} \min_{i=1,2} \tilde{Q}_{\tilde{\theta}'_{m,i}}(\tilde{\mathbf{x}}', \tilde{a}_1', \cdots, \tilde{a}_N'). \tag{46}$$

Utilizing the value function, the gradient descent method can be used to optimize the policy parameters of the agent m

$$\begin{aligned} \nabla_{\tilde{\theta}_{m,1}} J\left(\tilde{\phi}_m\right) = & \mathbb{E}_{\tilde{X}\sim\tilde{\mathcal{D}}} \Big[\nabla_{\tilde{\phi}_m} \tilde{\pi}_{\tilde{\phi}_m}(\tilde{a}_m \mid \tilde{o}_m) \cdot \nabla_{\tilde{a}_m} \\ & \tilde{Q}_{\tilde{\theta}_{m,1}}(\tilde{\mathbf{x}}, \tilde{a}_1, \cdots, \tilde{a}_N)\Big|_{\tilde{a}_m = \tilde{\pi}_{\tilde{\phi}_m}(\tilde{o}_m)} \Big], \end{aligned} \tag{47}$$

where $\tilde{\mathcal{D}}$ is the experience replay buffer for all agents.

Then train the Critic network with global information, using TD to reduce the difference between the current value and the target value, which can be expressed as

$$\mathcal{L}(\tilde{\theta}_{m,i}) = \mathbb{E}_{\tilde{\mathbf{x}},\tilde{a},\tilde{r},\tilde{\mathbf{x}}'} \left[\left(\tilde{Q}_{\tilde{\theta}_{m,i}}(\tilde{\mathbf{x}}, \tilde{a}_1, \cdots, \tilde{a}_N) - \tilde{y}_m \right)^2 \right]. \tag{48}$$

In order to smooth the strategy, Gaussian noise that be clipped is added to the Actor network, expressed as

$$\psi = \text{clip}(\overline{N}(0, \tilde{\sigma}), -\tilde{C}, \tilde{C}), \tag{49}$$

where $\overline{N}(0, \tilde{\sigma})$ denotes a Gaussian distribution with mean of 0 and standard deviation of $\tilde{\sigma}$, $\tilde{C}$ is a hyperparameter for the range of clip. Then the modified actions can be defined as

$$\tilde{a}_m = \tilde{\pi}_{\tilde{\phi}_m}(\tilde{o}_m) + \psi. \tag{50}$$

In addition, in order to have an accurate Critic network before the Actor network update, the MATD3 algorithm updates three target networks after each Critic update. The method of using soft updates to update the parameters of the target network can be expressed as

$$\begin{cases} \tilde{\phi}'_m \leftarrow \tau\tilde{\phi}_m + (1-\tau)\tilde{\phi}'_m, \\ \tilde{\theta}'_{m,i} \leftarrow \tau\tilde{\theta}_m + (1-\tau)\tilde{\theta}'_{m,i}, \end{cases} \tag{51}$$

where τ is soft update parameter. The complete AUV dynamic node selection algorithm process is summarized in Algorithm 3.

VI. Performance Evaluation

In this section, we provide the simulation setup and then verify the effectiveness of the proposed scheme.

A. Simulation Setup

To evaluate the proposed scheme, we consider a scenario where divers need to concentrate distribution due to some group tasks, so we randomly implement three AUVs within a 1000 m $\times$ 1000 m simulation area, and 20 divers are distributed in different regions according to different tasks. The simulations are based on Python 3.11, with hardware platforms for the 13th generation i9-13980HX and Nvidia 4060 processor. The main parameters are shown in Table 1.

TABLE I: Simulation Parameters.

Parameters	Description 2	Value
c	Extinction coefficient	$0.151(m^{-1})$
R	Responsivity of the photodiode	$0.28(A/W)$
D_R	Receiver aperture diameter	$0.15(m)$
B	Visible light communication bandwidth	$7 \times 10^5(kHz)$
P_T	Transmit power	$30(dBm)$
Δf	Underwater acoustic bandwidth	$2(kHz)$
f	Carrier frequency	$35(kHz)$
p_a	AUV transmission power	$0.3(W)$
p_u	USV transmission power	$1(W)$
H_d	Hidden layer dimension	64
H_n	Number of Hidden layers	2
λ	GAE parameter	0.95
P	Step number	15
$\lambda_{entropy}$	Strategy entropy weight	0.01
E	Traning episodes	3×10^5
L	Learn interval	32
γ	Discount factor	0.99
ϵ	The range of clip	0.2
κ	Policy update frequency	2
l_α	Actor learning rate	5×10^{-4}
l_c	Critic learning rate	5×10^{-4}
S	Batch size	32

B. The Effectiveness of the Assisted Diver Underwater Communication Method

To evaluate the communication performance between divers, we test the average BER_E between divers covered by the same AUV. As shown in Fig. 4(a), each curve represents the average BER_E between divers served by each AUV at each step. During the 200-step testing time, the BER_E between divers in the same cluster remained relatively stable. The BER_E is affected by the distribution of divers, the more concentrated the distribution of divers, the higher the BER_E. At the same time, the BER_E may be relatively high in the initial stage because the AUV is initialized to random positions within a predetermined range. We also tested the communication performance between divers in different clusters as shown in the Fig. 4(b). The curves represent the average BER_E of communication between divers covered by two different AUVs. The fluctuation and magnitude of the BER_E of the three curves are different, because the relative distance between the three AUVs is not the same. The closer distance between AUVs, the smaller and more stable the BER_E, and there is also a phenomenon where the initial BER_E is too high caused by random initialization.

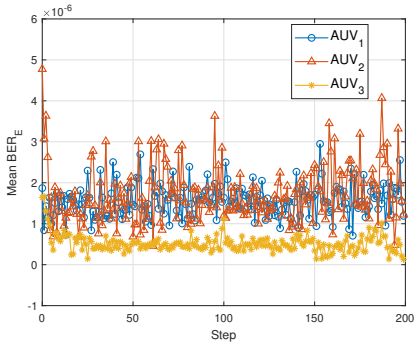

(a) Covered by the same AUV.

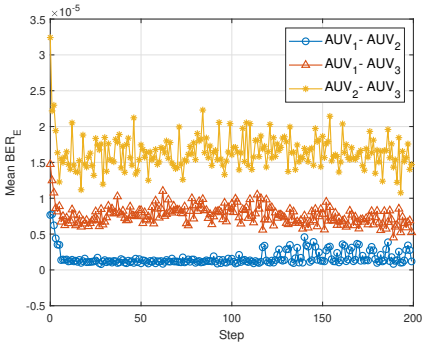

(b) Covered by the different AUV.

Fig. 4: The mean BER_E between divers.

We further evaluate the maximum data transmission rate of the VLC channel between divers. The curves in Fig. 5(a) represent the maximum data transmission rate between the divers served by the same AUV. It can be seen that at the beginning of the testing phase, the maximum data transmission rate rapidly increases and converges to a stable state with the cooperative movement of AUVs. The convergent rate can also be affected by the distribution of divers. The maximum data transmission rate between divers in different clusters is shown in Fig. 5(b), each curve in the figure represents the maximum data transmission rate between divers covered by two different AUVs. There are fluctuations at the beginning of the test for a period of time, and then it quickly converges to a stable

state. The convergent value of the data transmission rate is also related to the distance between AUVs.

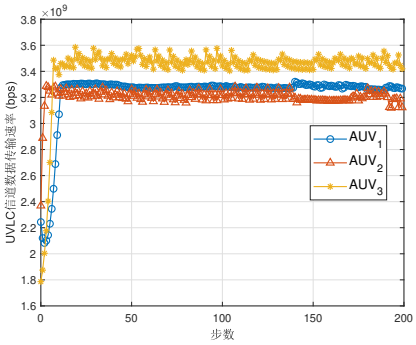

(a) Covered by the same AUV.

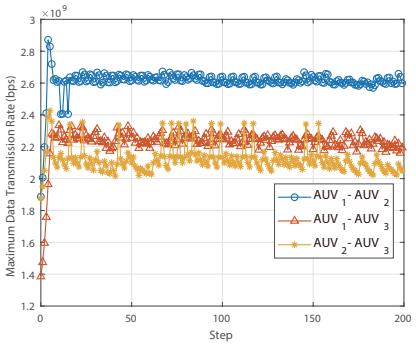

(b) Covered by the different AUV.

Fig. 5: The maximum data transmission rate of VLC between divers.

To further verify the VLC coverage of the proposed scheme, we compare it with the MADDPG [16] approach as shown in Fig. 6. Although the algorithm based on MADDPG can stabilize at around 40% in the initial stage, the AUV is difficult to adjust and move with divers' position change, resulting in large fluctuation and instability in coverage. The algorithm based on MAPPO can quickly stabilize to around 65% with smaller fluctuation, and can stably provide VLC coverage to divers.

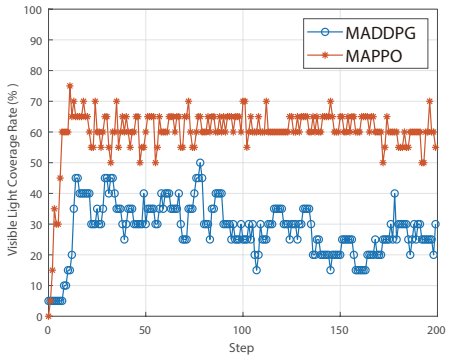

Fig. 6: The visible light coverage rate based on MAPPO and MADDPG algorithms.

To further demonstrate the effectiveness of the proposed scheme, we compared it with the method based on MADDPG as shown in Fig. 7. We combine MAPPO and MADDPG with K-medoids and K-means algorithm respectively. It can be seen that regardless of which clustering algorithm is used, the average distance between AUVs and centroids in the MAPPO algorithm is smaller and more stable, and the K-medoids algorithm performs better. This is because the MADDPG algorithm is based on deterministic policy gradient method, which may get stuck in local optimal solutions and make it difficult to find the global optimal policy.

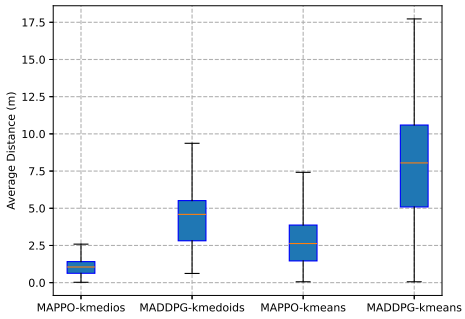

Fig. 7: The average distance to centroid based on MAPPO and MADDPG algorithms.

C. The Effectiveness of USV-AUV assisted communication method

The average transmission time from AUV to surface platform is shown in Figure 8. During the 200 steps testing period, the average transmission time of the three AUVs remained stable between 1.44 s - 1.5 s through dynamically collaborative selection of AUVs. There are some outliers in the figure. On the one hand, the RF link has Rayleigh fading, which can cause fluctuations in the transmission time between the USV relay node and the surface platform. On the other hand, there are differences in the amount of data of the AUV at different time slots. When the AUV data volume is excessive at a certain time slot, the transmission time will be too long. But overall it remains within a stable range and can meet the communication requirements between divers and the surface platform.

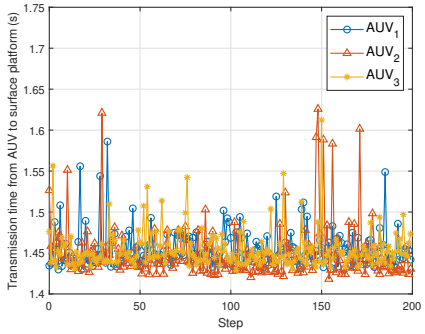

Fig. 8: The average transmission time from AUV to surface platform.

In order to demonstrate the performance of the proposed method under different AUV and USV quantities configurations, we propose three different AUV and USV quantities configuration schemes. As shown in Table III, the differences in communication performance among the three configuration schemes were compared. From the table, we can see that the three schemes maintain a stable range in terms of path loss, SNR, BER, and transmission energy consumption. However, as the number of AUVs and USVs increases, the overall performance also decreases to a certain extent. This phenomenon is mainly attributed to the deteriorating learning effectiveness of multi-agent reinforcement learning in the face of the increasing number of agents and expanding environmental dimensions.

TABLE II: Different configuration schemes

Quantity	Scheme 1	Scheme 2	Scheme 3
AUV quantities	3	4	5
USV quantities	6	8	10

TABLE III: Comparison of mean and standard deviation of communication performance for different configuration schemes

	PL		SNR		BER		EC	
	Mean	Std	Mean	Std	Mean	Std	Mean	Std
Scheme 1	22.08	0.53	20.86	0.43	2.5×10^{-6}	5.4×10^{-7}	408.14	14.02
Scheme 2	23.97	0.55	20.47	0.75	3.0×10^{-6}	6.4×10^{-7}	550.20	10.59
Scheme 3	24.68	0.67	20.14	0.65	3.6×10^{-6}	8.7×10^{-7}	690.62	16.19

To verify the reliability of cross-media communication, we also compared the SNR and BER in the communication between AUVs and surface platform, as shown in Figure 9. It can be seen that the average SNR of the proposed method is higher than that of other methods, and the BER is also lower than that of other methods. The MADDPG method suffers from the overestimation of deterministic strategies, leading to policy updates towards suboptimal directions. Especially in multi-agent environments, the collaboration and interaction among agents can exacerbate this overestimation, thereby affecting the convergence and final performance of the algorithm, which results in slightly inferior performance compared to the proposed method. The greedy method only selects the USV closest to an AUV, and there is a lack of collaborative strategies among AUVs. Therefore, the greedy and random methods perform poorly due to the lack of collaborative strategies.

We further conducted comparative experiments on the transmission energy consumption of cross-media communication. The performance of energy consumption also indirectly demonstrates the overall difference in transmission time. As shown in Figure 10, the proposed method has lower transmission energy consumption than other methods and is more stable. The strategy based on MADDPG may encounter suboptimal situations, so the overall transmission energy consumption will be slightly higher than the proposed method, and the distribution range will be larger. However, the greedy and random methods perform significantly worse than the previous two schemes in terms of performance, which further validate the effectiveness of the proposed method.

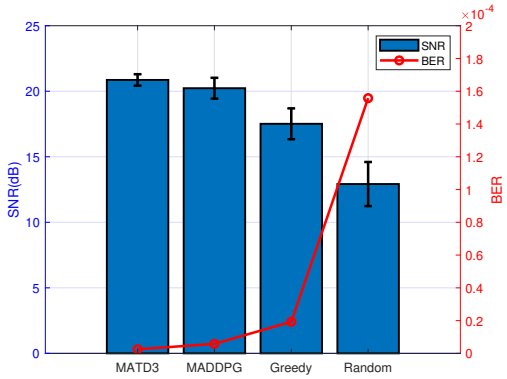

Fig. 9: The average SNR and BER form AUV to surface platform.

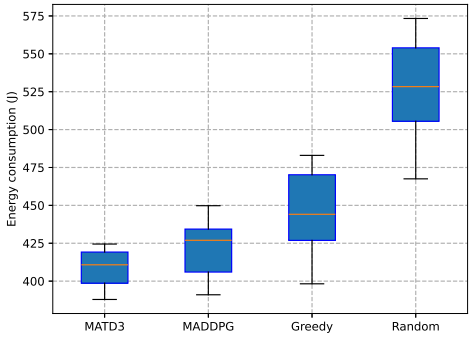

Fig. 10: The transmission energy consumption from AUV to surface platform.

VII. Conclusion

In this paper, we proposed a novel scheme that utilizes heterogeneous USV-AUV to assist divers in achieving high-speed and reliable communication. In this scheme, we first model the communication channels, and then using MAPPO algorithm combined with K-medoids to control AUV cooperative movement to solve the communication problem between divers. After that, we design an algorithm to control AUV adaptive selection of USV relay nodes based on MATD3, so as to maximize the cross-media communication rate of divers. Finally, through extensive simulations, we have verified the effectiveness of the proposed method.

References

[1] Đula Nađ, Filip Mandić, and Nikola Mišković. Using autonomous underwater vehicles for diver tracking and navigation aiding. *Journal of marine science and engineering*, 8(6):413–432, 2020.

[2] Hui-Min Chou, Yu-Cheng Chou, and Hsin-Hung Chen. Development of a monocular vision deep learning-based auv diver-following control system. In *Global Oceans 2020: Singapore–U.S. Gulf Coast*, pages 1–4, 2020.

[3] S Gunanandhini, G Manojkumar, M Ragul, S Manjit, R Gokul, et al. Scuba divers health monitoring and risk management system. In *2023 9th International Conference on Advanced Computing and Communication Systems (ICACCS)*, pages 1477–1481, 2023.

[4] Derek W Orbaugh Antillon, Christopher R Walker, Samuel Rosset, and Iain A Anderson. Glove-based hand gesture recognition for diver communication. *IEEE Transactions on Neural Networks and Learning Systems*, 34(12):9874–9886, 2022.

[5] Marco Bernardi, Christian Cardia, Petrika Gjanci, Andrea Monterubbiano, Chiara Petrioli, Luigi Picari, and Daniele Spaccini. The diver system: Multimedia communication and localization using underwater acoustic networks. In *2019 IEEE 20th International Symposium on" A World of Wireless, Mobile and Multimedia Networks"(WoWMoM)*, pages 1–8, 2019.

[6] Tong Zhang, Yu Gou, Jun Liu, and Jun-Hong Cui. Traffic load-aware resource management strategy for underwater wireless sensor networks. *IEEE Transactions on Mobile Computing*, pages 1–18, 2024.

[7] Alaa G Nasser and Mazin Ali A Ali. Performance of led for line-of-sight (los) underwater wireless optical communication system. *Journal of Optical Communications*, 44(s1):1355–1363, 2024.

[8] Hanjiang Luo, Jinglong Wang, Fanfeng Bu, Rukhsana Ruby, Kaishun Wu, and Zhongwen Guo. Recent progress of air/water cross-boundary communications for underwater sensor networks: A review. *IEEE Sensors Journal*, 22(9):8360–8382, 2022.

[9] Syed Agha Hassnain Mohsan, Abid Hussain, Nawaf Qasem Hamood Othman, and Hussain Amjad. Investigation and design of laser diode based diver-to-diver optical communication system. In *2020 IEEE MTT-S International Conference on Numerical Electromagnetic and Multiphysics Modeling and Optimization (NEMO)*, pages 1–4, 2020.

[10] Jesse R. Pelletier, Brendan W. O'Neill, John J. Leonard, Lee Freitag, and Eric Gallimore. Auv-assisted diver navigation. *IEEE Robotics and Automation Letters*, 7(4):10208–10215, 2022.

[11] Hanjiang Luo, Xu Wang, Fanfeng Bu, Yuting Yang, Rukhsana Ruby, and Kaishun Wu. Underwater real-time video transmission via wireless optical channels with swarms of auvs. *IEEE Transactions on Vehicular Technology*, 72(11):14688–14703, 2023.

[12] Ling Lyu, Cailian Chen, Shanying Zhu, and Xinping Guan. 5g enabled codesign of energy-efficient transmission and estimation for industrial iot systems. *IEEE Transactions on Industrial Informatics*, 14(6):2690–2704, 2018.

[13] Wei Wei, Jingjing Wang, Zhengru Fang, Jianrui Chen, Yong Ren, and Yuhan Dong. 3u: Joint design of uav-usv-uuv networks for cooperative target hunting. *IEEE Transactions on Vehicular Technology*, 72(3):4085–4090, 2022.

[14] Hui Zeng, Zhou Su, Qichao Xu, and Dongfeng Fang. Usv fleet-assisted collaborative data backup in marine internet of things. *IEEE Internet of Things Journal*, pages 36308–36321, 2024.

[15] Jingjing Wang, Shuai Liu, Wei Shi, Guangjie Han, and Shefeng Yan. A multi-auv collaborative ocean data collection method based on lg-dqn and data value. *IEEE Internet of Things Journal*, 11(5):9086–9106, 2023.

[16] Ryan Lowe, Yi I Wu, Aviv Tamar, Jean Harb, OpenAI Pieter Abbeel, and Igor Mordatch. Multi-agent actor-critic for mixed cooperative-competitive environments. *Advances in neural information processing systems*, 30:6382–6393, 2017.

[17] Jingyi He, Meng Xi, Jiabao Wen, Shuai Xiao, and Jiachen Yang. Marl-based auv formation for underwater intelligent autonomous transport systems supported by 6g network. *IEEE Transactions on Intelligent Transportation Systems*, pages 1–10, 2024.

[18] Chao Yu, Akash Velu, Eugene Vinitsky, Jiaxuan Gao, Yu Wang, Alexandre Bayen, and Yi Wu. The surprising effectiveness of ppo in cooperative multi-agent games. *Advances in Neural Information Processing Systems*, 35:24611–24624, 2022.

[19] Johannes Ackermann, Volker Gabler, Takayuki Osa, and Masashi Sugiyama. Reducing overestimation bias in multi-agent domains using double centralized critics. *arXiv preprint arXiv:1910.01465*, pages 1–10, 2019.

[20] Chelsey Edge and Junaed Sattar. Diver interest via pointing: Human-directed object inspection for auvs. In *2023 IEEE International Conference on Robotics and Automation (ICRA)*, pages 3146–3153, 2023.

[21] Chettiyar Vani Vivekanand, TM Inbamalar, B Kavimani, et al. Remote health monitoring of divers using underwater acoustic communication. In *2023 International Conference on Recent Advances in Electrical, Electronics, Ubiquitous Communication, and Computational Intelligence (RAEEUCCI)*, pages 1–6, 2023.

[22] Prasad Anjangi, Amy Gibson, Manu Ignatius, Chinmay Pendharkar, Anne Kurian, Alan Low, and Mandar Chitre. Diver communication and localization system using underwater acoustics. In *Global Oceans 2020: Singapore–US Gulf Coast*, pages 1–8, 2020.

[23] Hanjiang Luo, Saisai Ma, Hang Tao, Rukhsana Ruby, Jiehan Zhou, and Kaishun Wu. Drl-optimized optical communication for a reliable uav-based maritime data transmission. *IEEE Internet of Things Journal*, 11(10):18768–18781, 2024.

[24] Yuan Zhang, Zixian Wei, Zhongxu Liu, Chen Cheng, Zhaoming Wang, Xinke Tang, Yanfu Yang, Changyuan Yu, and HY Fu. Optical communication and positioning convergence for flexible underwater wireless sensor network. *Journal of Lightwave Technology*, 41(16):5321–5327, 2023.

[25] Cheng Zeng, Jun-Bo Wang, Changfeng Ding, Hua Zhang, Min Lin, and Julian Cheng. Joint optimization of trajectory and communication resource allocation for unmanned surface vehicle enabled maritime wireless networks. *IEEE Transactions on Communications*, 69(12):8100–8115, 2021.

[26] Jun-Bo Wang, Cheng Zeng, Changfeng Ding, Hua Zhang, Min Lin, and Jiangzhou Wang. Unmanned surface vessel assisted maritime wireless communication toward 6g: Opportunities and challenges. *IEEE Wireless Communications*, 29(6):72–79, 2022.

[27] Na Su, Jun-Bo Wang, Cheng Zeng, Hua Zhang, Min Lin, and Geoffrey Ye Li. Unmanned-surface-vehicle-aided maritime data collection using deep reinforcement learning. *IEEE Internet of Things Journal*, 9(20):19773–19786, 2022.

[28] Zheng Hu, Zhou Su, and Qichao Xu. Usv-aided data secure collection scheme for underwater wireless acoustic networks. In *GLOBECOM 2023-2023 IEEE Global Communications Conference*, pages 7157–7162. IEEE, 2023.

[29] Yufeng Han, Yue Xiao, Yulan Gao, Mingming Wu, and Binhong Dong. Dynamic relay selection for usv-aided smart ocean iot. *IEEE Communications Letters*, pages 1723–1727, 2024.

[30] Mohammed Elamassie, Farshad Miramirkhani, and Murat Uysal. Performance characterization of underwater visible light communication. *IEEE Transactions on Communications*, 67(1):543–552, 2018.

[31] Nils Morozs, Wael Gorma, Benjamin T. Henson, Lu Shen, Paul D. Mitchell, and Yuriy V. Zakharov. Channel modeling for underwater acoustic network simulation. *IEEE Access*, 8:136151–136175, 2020.

[32] Ling Lyu, Yanpeng Dai, Nan Cheng, Shanying Zhu, Xinping Guan, Bin Lin, and Xuemin Shen. Aoi-aware co-design of cooperative transmission and state estimation for marine iot systems. *IEEE Internet of Things Journal*, 8(10):7889–7901, 2020.

[33] Zhongwei Shen, Hongxi Yin, Lianyou Jing, Xiuyang Ji, Yanjun Liang, and Jianying Wang. A power control-aided q-learning-based routing protocol for optical-acoustic hybrid underwater sensor networks. *IEEE Transactions on Green Communications and Networking*, 7(4):2117–2129, 2023.

[34] Yang Weng, Yuki Sekimori, Sehwa Chun, Omar Alkhazragi, Takumi Matsuda, Abderrahmen Trichili, Tien Khee Ng, Boon S Ooi, and Toshihiro Maki. Scalable laser-based underwater wireless optical communication solution between autonomous underwater vehicle fleets. *Applied Optics*, 62(31):8261–8271, 2023.

[35] Fang Li and Caifang Wang. Develop a multi-linear-trend fuzzy information granule based short-term time series forecasting model with k-medoids clustering. *Information Sciences*, 629:358–375, 2023.

[36] Wenqiang Cao, Jing Yan, Xian Yang, and Xiaoyuan Luo. Reinforcement learning-based formation control of autonomous underwater vehicles with model interferences. In *2021 40th Chinese Control Conference (CCC)*, pages 4020–4025, 2021.

[37] Jiangliang Jin and Yunjian Xu. Optimal policy characterization enhanced proximal policy optimization for multitask scheduling in cloud computing. *IEEE Internet of Things Journal*, 9(9):6418–6433, 2021.

[38] Hualei Zhang, Jun Du, Chunxiao Jiang, Aymen Fakhreddine, Ahmed Alhammadi, and Jintao Wang. Matd3-based joint user association and resource allocation in uav networks. In *GLOBECOM 2023-2023 IEEE Global Communications Conference*, pages 6892–6897. IEEE, 2023.